Moreau et al., http://www.jgp.org/cgi/content/full/jgp.201411304/DC1

The PDB files are available for download as a ZIP file and represent the models of $Na_v1.5$ WT or mutant channels (R222Q and R225W) at different states, at the end of the molecular dynamics simulation process. WT channel is shown at both β and γ states (Nav15_DI_β_WT and Nav15_DI_gamma_WT, respectively). $Na_v1.5$ R222Q channel is shown in the γ state (Nav15_DI_gamma_R222Q). $Na_v1.5$ R225W channel is shown in the β state (Nav15_DI_β_R225W). All PDBs contain the complete system, including the protein, lipids, water molecules, and ions.

Figure S1. Sequence alignments used to build the homology model. The alignments of the S4 segments used to build the homology model in three states (α, β, and γ) are presented. Positive gating charges are highlighted in blue, and negative charges are highlighted in red.

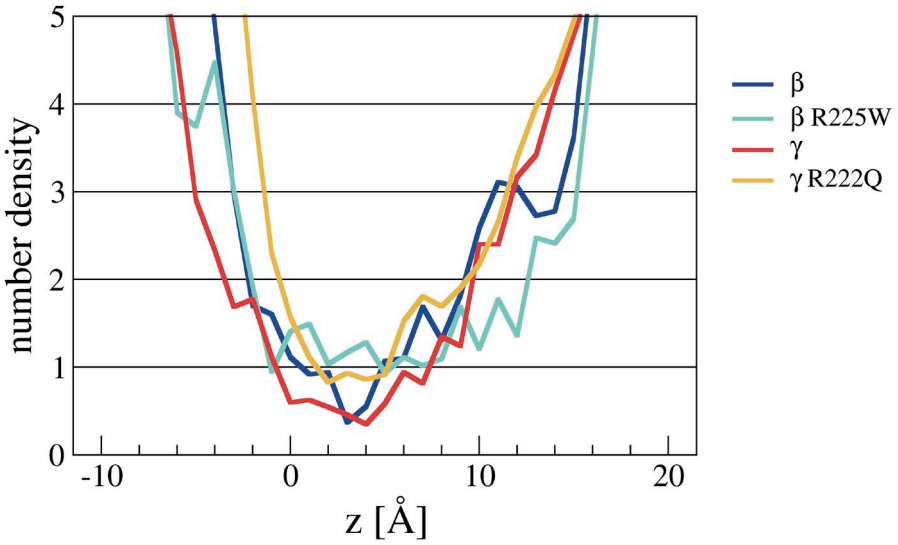

Figure S2. Water density profiles of the $Na_v1.5$ WT and mutant channels. Water density profiles along the main axis of the VSD in the β and γ WT channels (dark blue and red) and the β R225W mutant (light blue) and γ R222Q mutant channels (orange). The histograms were built using a 1-Å grid, and the averages were calculated from the last 10 ns of the trajectories. 0 corresponds to the position of the Cα of Y168 of S2. Note that, for the WT system, the water number density is <1 at the constriction, indicating a disruption of the water-accessible volume. For the two mutants, however, the water density remains at or above one molecule, indicating a continuous water-accessible volume bridging the internal and external crevices.

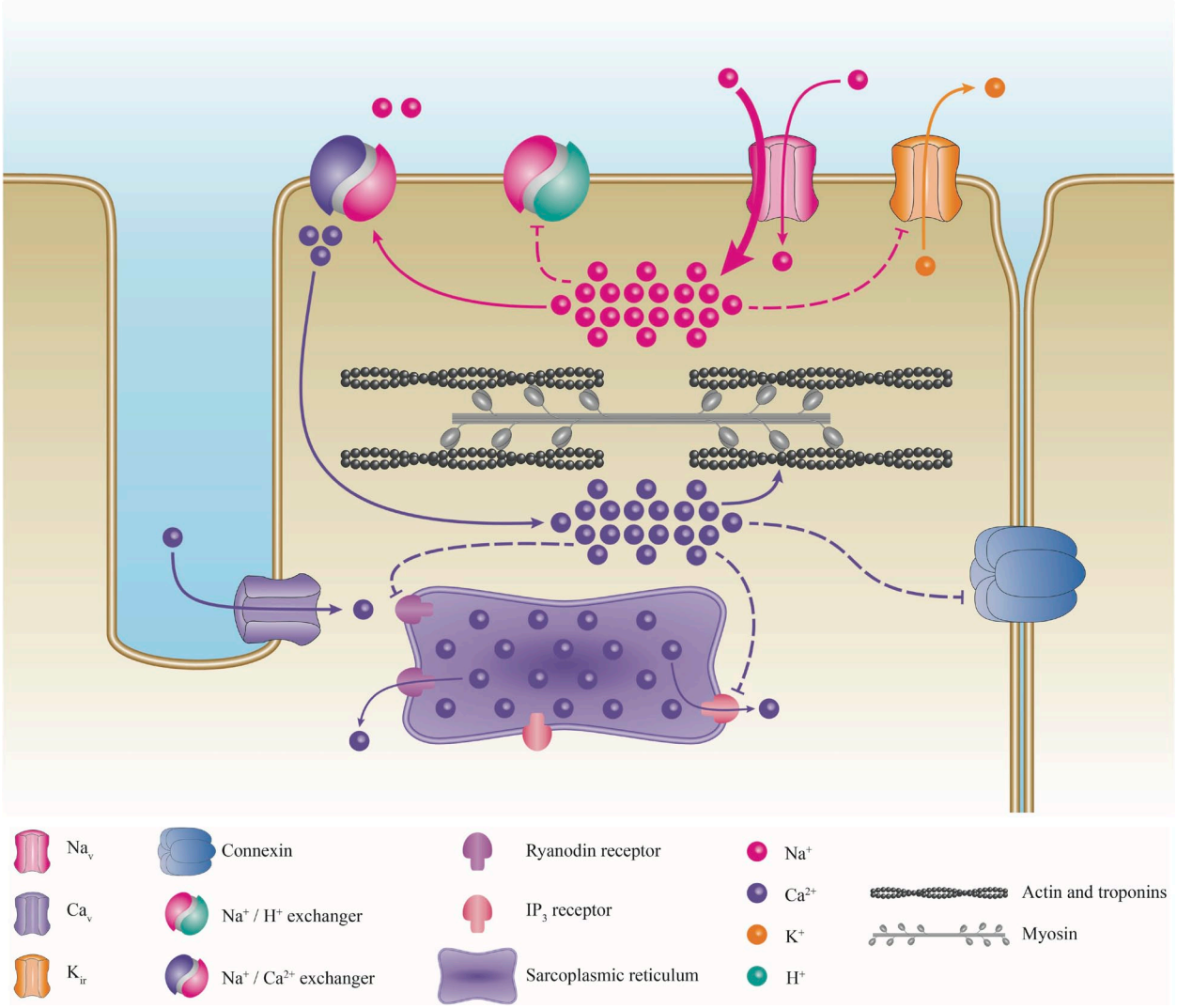

Figure S3. Proposed pathological mechanism. Schematic representation of a myocyte with its main ion channels and exchangers. The contractile proteins, sarcoplasmic reticulum, and connexins are shown in gray, purple, and blue, respectively. The appearance of a gating pore current induces an ionic homeostasis imbalance by the activation of several exchangers. The bold pink arrow representing the Na^+ leak indicates the start point. Figure adapted from Moreau et al. (2014).

TABLE S1

Divergent biophysical properties of the R222Q and R225W mutations, which have similar clinical phenotypes

Mutation	Study	Biophysical defect						Clinical phenotype		
		Current density	Activation	Inactivation	Recovery	Kinetics	Window	Atrial	Conduction system	Ventricular
			mV	*mV*						
R222Q[a]	Cheng et al., 2010	↓	−13	−4	Slow	≈	≈	AFib, PAC	AVB, BBB, CSD	PVC
	McNair et al., 2011	ND	ND	ND	ND	ND	ND	AFib		Tach, PVC
	Nair et al., 2012	≈	−9	−7.3	≈	I slow	↑	AFib	AVB	Tach
	Laurent et al., 2012	≈	−11.7	−5	≈	A Fast, I Fast	↑	AFib, PAC, AFL	AVB, BBB	Tach, PVC
	Mann et al., 2012	≈	−6.3	−6.2	Slow	≈	↑	AFib, PAC, Brad	BBB	PVC
R225W[a]	Bezzina et al., 2003	↓	14	11	≈	≈	ND		AVB	Tach

↑, increase; ↓, decrease; ≈, not impacted; A Fast, faster activation kinetics; AFib, atrial fibrillation; AFL, atrial flutter; A Slow, slower activation kinetics; AVB, first, second, or third degree atrio-ventricular block; BBB, incomplete right or left bundle branch block; Brad, bradycardia; CSD, conduction system disease; I Fast, faster inactivation kinetics; I Slow, slower inactivation kinetics; ND, not determined; PAC, premature atrial contractions; PVC, premature ventricular contractions; Tach, tachycardia divergences reported in the biophysical properties of the R222Q channel (current density, window current, recovery from inactivation, and current kinetics) have been proposed to be caused by the presence of the H558R polymorphism and the different heterologous expression systems used to study these properties (*Xenopus laevis* oocytes, HEK293, COS, and CHO cells).

[a]The hypothesis of arrhythmia-induced cardiomyopathy seems unlikely. Indeed, for both mutations the age of onset is relatively young (the diagnostic is often before 21 yr, with some cases at 7 yr). Furthermore a patient of <1 yr of age has been described (27). The periods of arrhythmias before death of this patient were of short duration, minimizing the probability of arrhythmia-induced dilatation.

TABLE S2

Schematic salt-bridge network pattern in the models of the three different conformations of the WT $Na_v1.5$ DI domain

α	PO4- (top)	E1 (S2)	D2 (S3)	E3 (S2)	PO4- (bottom)
R1 (R219)	X				
R2 (R222)	X	X			
R3 (R225)		X			
K4 (K228)			X	X	
β					
R1 (R219)	X	X			
R2 (R222)		X			
R3 (R225)			X	X	
γ					
R1 (R219)		X			
R2 (R222)			X	X	
R3 (R225)				X	X
K4 (K228)					X

REFERENCES

Bezzina, C.R., M.B. Rook, W.A. Groenewegen, L.J. Herfst, A.C. van der Wal, J. Lam, H.J. Jongsma, A.A. Wilde, and M.M. Mannens. 2003. Compound heterozygosity for mutations (W156X and R225W) in SCN5A associated with severe cardiac conduction disturbances and degenerative changes in the conduction system. *Circ. Res.* 92:159–168. http://dx.doi.org/10.1161/01.RES.0000052672.97759.36

Cheng, J., A. Morales, J.D. Siegfried, D. Li, N. Norton, J. Song, J. Gonzalez-Quintana, J.C. Makielski, and R.E. Hershberger. 2010. SCN5A rare variants in familial dilated cardiomyopathy decrease peak sodium current depending on the common polymorphism H558R and common splice variant Q1077del. *Clin. Transl. Sci.* 3:287–294. http://dx.doi.org/10.1111/j.1752-8062.2010.00249.x

Laurent, G., S. Saal, M.Y. Amarouch, D.M. Béziau, R.F. Marsman, L. Faivre, J. Barc, C. Dina, G. Bertaux, O. Barthez, et al. 2012. Multifocal ectopic Purkinje-related premature contractions: A new SCN5A-related cardiac channelopathy. *J. Am. Coll. Cardiol.* 60:144–156. http://dx.doi.org/10.1016/j.jacc.2012.02.052

Mann, S.A., M.L. Castro, M. Ohanian, G. Guo, P. Zodgekar, A. Sheu, K. Stockhammer, T. Thompson, D. Playford, R. Subbiah, et al. 2012. R222Q SCN5A mutation is associated with reversible ventricular ectopy and dilated cardiomyopathy. *J. Am. Coll. Cardiol.* 60:1566–1573. http://dx.doi.org/10.1016/j.jacc.2012.05.050

McNair, W.P., G. Sinagra, M.R. Taylor, A. Di Lenarda, D.A. Ferguson, E.E. Salcedo, D. Slavov, X. Zhu, J.H. Caldwell, and L. Mestroni, and Familial Cardiomyopathy Registry Research Group. 2011. SCN5A mutations associate with arrhythmic dilated cardiomyopathy and commonly localize to the voltage-sensing mechanism. *J. Am. Coll. Cardiol.* 57:2160–2168. http://dx.doi.org/10.1016/j.jacc.2010.09.084

Moreau, A., P. Gosselin-Badaroudine, and M. Chahine. 2014. Biophysics, pathophysiology, and pharmacology of ion channel gating pores. *Front Pharmacol.* 5:53. http://dx.doi.org/10.3389/fphar.2014.00053

Nair, K., R. Pekhletski, L. Harris, M. Care, C. Morel, T. Farid, P.H. Backx, E. Szabo, and K. Nanthakumar. 2012. Escape capture bigeminy: Phenotypic marker of cardiac sodium channel voltage sensor mutation R222Q. *Heart Rhythm.* 9:1681–1688. http://dx.doi.org/10.1016/j.hrthm.2012.06.029